NANO LETTERS

Letter

pubs.acs.org/NanoLett

Fast Diagnostics of BRAF Mutations in Biopsies from Malignant Melanoma

François Huber,*[,†] Hans Peter Lang,[†] Katharina Glatz,[‡] Donata Rimoldi,[§] Ernst Meyer,[†] and Christoph Gerber*[,†]

[†]Swiss Nanoscience Institute, Department of Physics, University of Basel, CH-4056 Basel, Switzerland

[‡]Institute of Pathology, University Hospital Basel, CH-4031 Basel, Switzerland

[§]Ludwig Center for Cancer Research, University of Lausanne, CH-1066 Epalinges, Switzerland

Supporting Information

ABSTRACT: According to the American skin cancer foundation, there are more new cases of skin cancer than the combined incidence of cancers of the breast, prostate, lung, and colon each year, and malignant melanoma represents its deadliest form. About 50% of all cases are characterized by a particular mutation $BRAF^{V600E}$ in the BRAF (Rapid Acceleration of Fibrosarcoma gene B) gene. Recently developed highly specific drugs are able to fight $BRAF^{V600E}$ mutated tumors but require diagnostic tools for fast and reliable mutation detection to warrant treatment efficiency. We completed a preliminary clinical trial applying cantilever array sensors to demonstrate identification of a $BRAF^{V600E}$ single-point mutation using total RNA obtained from biopsies of metastatic melanoma of diverse sources (surgical material either frozen or fixated with formalin and embedded in paraffin). The method is faster than the standard Sanger or pyrosequencing methods and comparably sensitive as next-generation sequencing. Processing time from biopsy to diagnosis is below 1 day and does not require PCR amplification, sequencing, and labels.

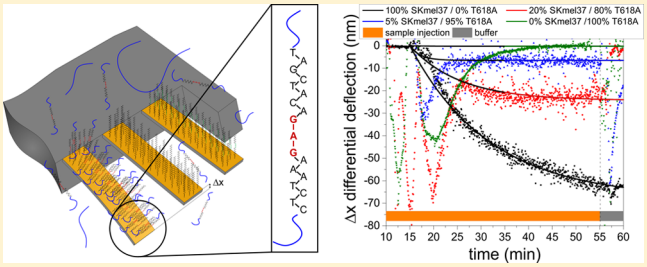

KEYWORDS: *Nanomechanical microcantilever, biosensor, malignant melanoma, skin cancer*

Cancer is the number one cause of death worldwide surpassing cardiovascular disease or all strokes.[1] The most common malignancy in humans is skin cancer.[2] The occurrence of cutaneous malignant melanoma has steadily increased over the past 50 years in fair-skinned populations and still grows in many developed countries as a result of changing sun-seeking behavior. Only up to 5% of all skin cancers are malignant melanomas, but they are responsible for almost all fatalities. However, recently novel treatment methods have been developed. They are based on compounds with high specificity that have initiated stratified healthcare therapies by targeting particular driver mutations in various genes, e.g., BRAF (Rapid Acceleration of Fibrosarcoma gene B) inhibitors like vemurafenib for patients with $BRAF^{V600E}$ mutated tumors.[3,4] In combination with new mitogen-activated protein kinase kinase (MAP2K, MEK, MAPKK) inhibitors such as cobimetinib,[5] life expectancy can be extended to about one year[6] with fewer side effects than the standard chemotherapeutic drug dacarbazine. The current gold standard for mutation screening in malignant tumors uses real-time polymerase chain reaction (PCR) and sequencing methods for DNA extracted from biopsies. Our method neither needs PCR, nor labeling, nor sequencing. PCR protocols can be error-prone with false positives as a particular hazard. Artifacts complicate protocols[7] and extend processing time. We use an array of nanomechanical microcantilevers for surface stress sensing based on atomic force microscopy[8] to analyze DNA/DNA hybridization.[9−12] The technique was further adapted to reveal antigen/antibody,[13,14] transcription factor/DNA interactions,[15] and effects of antibiotics on bacteria.[16] The platform also proved applicability to study transcriptional activity of genes[17,18] and is able to characterize function of transmembrane protein activity.[19] Here, we report on the detection of the $BRAF^{V600E}$ mutation present in a subset of 50−60% malignant melanomas in human biopsies at the RNA level. We chose to use RNA since more RNA transcripts occur in the cytoplasm than genomic DNA counterparts. Moreover, RNA/DNA heterodimers have a higher thermodynamic stability than DNA/DNA homodimers. The hybrid double helix shows an increased hydrodynamic radius (DNA/DNA 1.07 ± 0.03 nm vs RNA/DNA 1.27 ± 0.03 nm),[20] which should result in a higher stress on the cantilever's surface due to steric hindrance, thereby increasing the sensitivity of the technique. Different oligonucleotides were designed to uniquely recognize the altered BRAF sequence. Searching the human genome expressed sequence tags database,[21] an 18 base sequence was chosen to detect unambiguously the BRAF

Received: April 12, 2016
Revised: July 28, 2016
Published: August 4, 2016

DOI: 10.1021/acs.nanolett.6b01513
Nano Lett. 2016, 16, 5373−5377

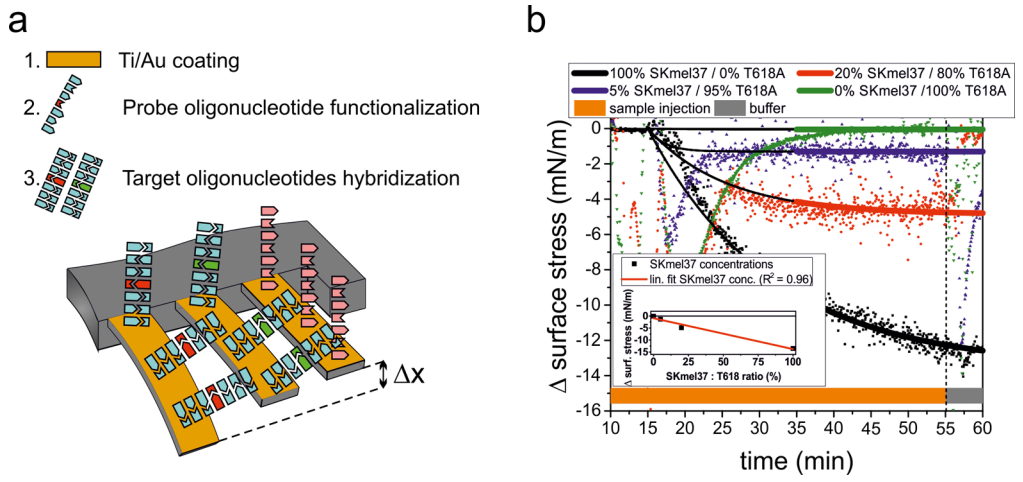

Figure 1. Schematic of a cantilever array demonstrating surface modifications for the detection of BRAF RNA. (a) Steps: 1. Coating eight cantilevers with Ti (adhesion layer) and Au for functionalization with thiols; 2. Adsorption of oligonucleotides for mutation recognition (site of mutation shown in red), wild type detection as a control (wild type site in green), or as nonspecific reference (polyAC; pink); 3. Experiment: total RNA injection containing complementary target sequences. Light blue indicates nonrelated sequences. The probe cantilevers will bend on hybridization depending on the presence of the mutation or the wild type or both, yielding a differential deflection Δx. All measurements must be done in a differential way to get reliable results, allowing us to exclude undesired influences from temperature and nonspecific adsorption. (b) Assessing the minimum RNA concentration for $BRAF^{V600E}$ detection using samples from cell lines: Various ratios of SK-Mel-37 $BRAF^{V600E}$ positive to T618A $BRAF^{V600E}$ negative total RNA (0%, 5%, 20%, and 100%) have been used. We superimposed Langmuir isotherms ($R^2 > 0.94$) on top of the data including the first 20 min dominated by mixing effects. The inset shows that the extrapolated differential deflections scale with the SK-Mel-37 concentrations.

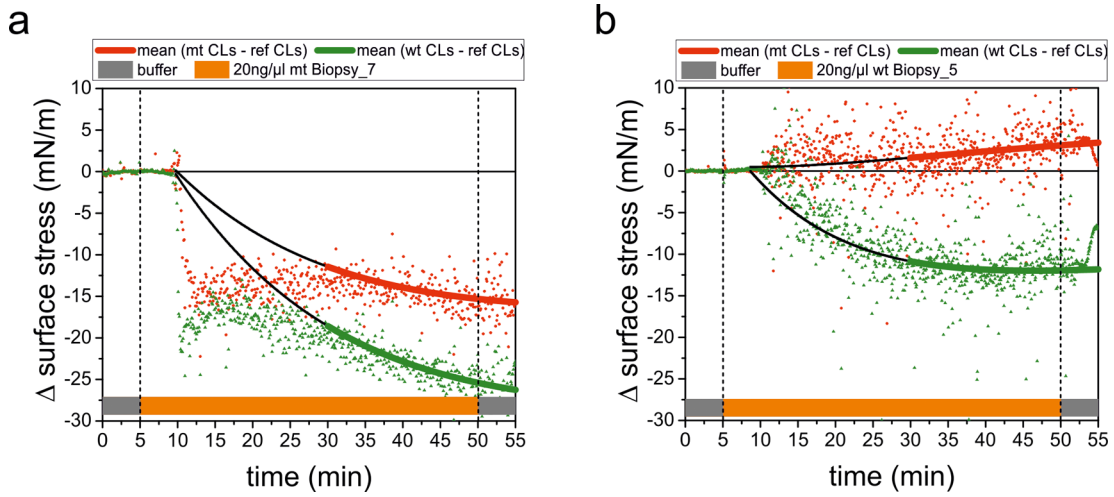

Figure 2. RNA samples from two biopsies are investigated. The red curve represents the difference of responses between mutant probe (mt) and polyAC reference cantilever (ref) implying presence of $BRAF^{V600E}$. The green curve shows a combination of wt reference and polyAC reference cantilevers indicating wild type BRAF. (a) $BRAF^{V600E}$ positive Biopsy_7 exhibiting a nonzero signal (red curve). (b) $BRAF^{V600E}$ negative Biopsy_5 showing a signal around zero in the red curve (for biopsy numbers and origin see Table 1). Langmuir fits ($R^2 > 0.95$) are superimposed on top of the data.

mRNA transcript. Our array sensor device facilitates addressing other mutations such as $BRAF^{V600K}$ for a more thorough investigation of tumors.

The working principle of nanomechanical microcantilever biosensors is depicted in a schematic way in Figure 1a and in an experimental setup in the Supporting Information, Figure S1. A self-assembled monolayer (SAM) of thiol-modified probe oligonucleotides (Supporting Information, Table S1) is covalently bound to gold-coated surfaces of the cantilevers. Upon hybridization with target oligonucleotides, bending of cantilevers is observed due to steric and ionic repulsion forces. Initial experiments to determine optimized hybridization conditions were performed (Supporting Information, Figure S2) in order to estimate the lowest ratio of mutant to wild type BRAF RNA (Figure 1b) required to conclusively identify the mutation by measuring various ratios.

The following two melanoma cell lines were selected (Ludwig Institute for Cancer Research, Univ. Lausanne): T618A carrying wild type BRAF and SK-Mel-37 carrying $BRAF^{V600E}$. The T618A line expresses a wild type form of BRAF, whereas the SK-Mel-37 line expresses the $BRAF^{V600E}$ mutant, and—to a lower extent—the wild type allele. Samples of total RNA obtained from two melanoma cell lines were mixed at different ratios and injected into the measurement chamber at a concentration of 20 ng/μL. The lowest ratio of 5% mutant in total wild type RNA turned out to be sufficient to identify the mutation in total RNA extracted from cell lines. A fraction of 5% is comparable to the amount other current

DOI: 10.1021/acs.nanolett.6b01513
Nano Lett. 2016, 16, 5373−5377

Table 1. Clinical Sample Analysis[a]

number	type of biopsy	origin	RNA yield. (μg)	RNA conc. (ng/μL)	BRAF status pathology	BRAF evaluation cantilever	% tumor cells as determined in pathology
Biopsy_1	FFPE	lung metastasis	9.4	188	mutant	mutant	95%
Biopsy_2	frozen	mesenteric metastasis	48.45	969	wild type	wild type	90%
Biopsy_3	FFPE	mesenteric metastasis	78.15	1563	wild type	wild type	not done
Biopsy_4	frozen	axillary lymph node metastasis	11.7	234	wild type	wild type	whole slide: 50%; marked area: 95%
Biopsy_5	FFPE	axillary lymph node metastasis	417	8340	wild type	wild type	not done
Biopsy_6	FFPE	cutaneous metastasis	626.95	12539	mutant	mutant	whole slide: 95%; marked area: 98%
Biopsy_7	FFPE	lymph node metastasis	94.2	1885	mutant	mutant	marked area: 98%
Biopsy_8	FFPE	axillary lymph node metastasis	133.2	2666	wild type	wild type	marked area: 98%
Biopsy_9	FFPE	pleural metastasis	39.5	792	mutant	mutant	marked area: 98%

[a]Total RNA was extracted from formalin-fixed paraffin-embedded tissue (FFPE) or frozen tumor samples. The RNA yield as well as the percentage of tumor cells estimated by a pathologist and total RNA concentrations of each biopsy are displayed. Three biopsies were additionally characterized by next generation sequencing (Biopsy_2, Biopsy_4, and Biopsy_8).

methods require such as the COBAS test[22] and represents a 4-fold improvement over standard PCR/sequencing.

Having established the conditions for $BRAF^{V600E}$ detection in different cell lines, the next step is to extend the investigation to biopsies of melanoma patients by performing a clinical pilot study comprising nine patients (Pathology Department of the University Hospital Basel). Two representative measurements are shown from $BRAF^{V600E}$ positive (Figure 2a) and from $BRAF^{V600E}$ negative (Figure 2b) melanoma biopsies. Melanoma tumors can be very heterogeneous with respect to their tumor cell expression profiles[23] and may contain variable levels of normal cells (Table 1). We obtained a large signal of −15 mN/m (red curve) in a $BRAF^{V600E}$ positive tumor biopsy (Figure 2a) in contrast to a small signal of +3.0 mN/m in a $BRAF^{V600E}$ negative tumor biopsy (Figure 2b). A large response (red curve) of the $BRAF^{V600E}$ detecting cantilever is a clear indicator for the presence of the $BRAF^{V600E}$ mutation, whereas the green curve does not interrogate $BRAF^{V600E}$. We observed a substantial signal of −25 mN/m for wild type BRAF (green curve) as the $BRAF^{V600E}$ positive melanoma also expresses the wild type allele to a large extent. Therefore, the presence of $BRAF^{V600E}$ is unambiguously verified in the $BRAF^{V600E}$ positive tumor biopsy sample. We performed nine analyses on human malignant melanoma biopsies (Biopsy_1 to Biopsy_9), as well as 21 analyses on tissue cultures (TC) $BRAF^{V600E}$ positive (10 samples, labeled TC_1 to TC_10) and negative cell lines (11 samples, labeled TC_11 to TC_21). Samples originated from formaldehyde-fixed, paraffin-embedded, FFPE, and frozen tissues.

We processed the data in a hierarchical cluster analysis (Figure 3 and Methods in Supporting Information) and were able to distinguish results obtained on cell lines and clinical samples (with the mutation in red and without the mutation in green). The dendrogram (tree structure) calculated using the method of Euclidian distances shows a bifurcation that reveals two main clusters representing mutant and wild type samples in both cell lines and clinical samples. The $BRAF^{V600E}$ positive biopsies are clearly part of the mutation cluster, and the $BRAF^{V600E}$ negative biopsies are part of the wild type cluster, manifesting the single point mutation sensitivity of our method. The fact that $BRAF^{V600E}$ biopsies and the different preparations of tissue culture samples bifurcate earlier (*) than the wild type biopsies and the corresponding tissue culture preparations do

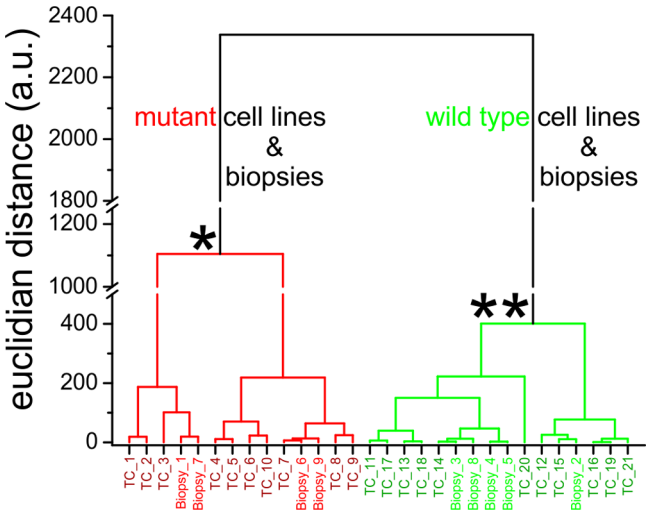

Figure 3. Hierarchical cluster analysis including 10 $BRAF^{V600E}$ positive tissue culture samples (TC_1 to TC_10, red), 11 $BRAF^{V600E}$ negative tissue culture samples (TC_11 to TC_21, green), and 9 biopsies (Biopsy_1 to Biopsy_9). The $BRAF^{V600E}$ positive biopsies 1, 6, 7, and 9 (red) are clearly distinguished from the $BRAF^{V600E}$ negative 2, 3, 4, 5, and 8 biopsies (green).

(**) reflects a higher variability in the biopsies. The $BRAF^{V600E}$ positive biopsies are parts of two different branches of the bifurcation (*). Biopsy_1 and Biopsy_7 are part of one branch, whereas Biopsy_6 and Biopsy_9 are members of the second branch. In contrast, the majority of the wild type biopsies including Biopsy_3, 8, 4, and 5 belong to the same branch of bifurcation (**), and only Biopsy_2 is a member of the other branch. These findings point toward a genetically more heterogeneous nature of the $BRAF^{V600E}$ biopsies and tissue culture samples as compared to the BRAF wild type biopsies and tissue cultures. A probable explanation is that different expression levels in the various samples influence the differential deflection signals. For comparison of our observations with the histological and sequencing findings we compiled Table 1 showing the state, origin, and type of biopsies. Our results agree with those obtained with standard methods of amplification and sequencing. In addition, our method provides high sensitivity, requiring only 5% of cancer cells in the sample

DOI: 10.1021/acs.nanolett.6b01513
Nano Lett. 2016, 16, 5373−5377

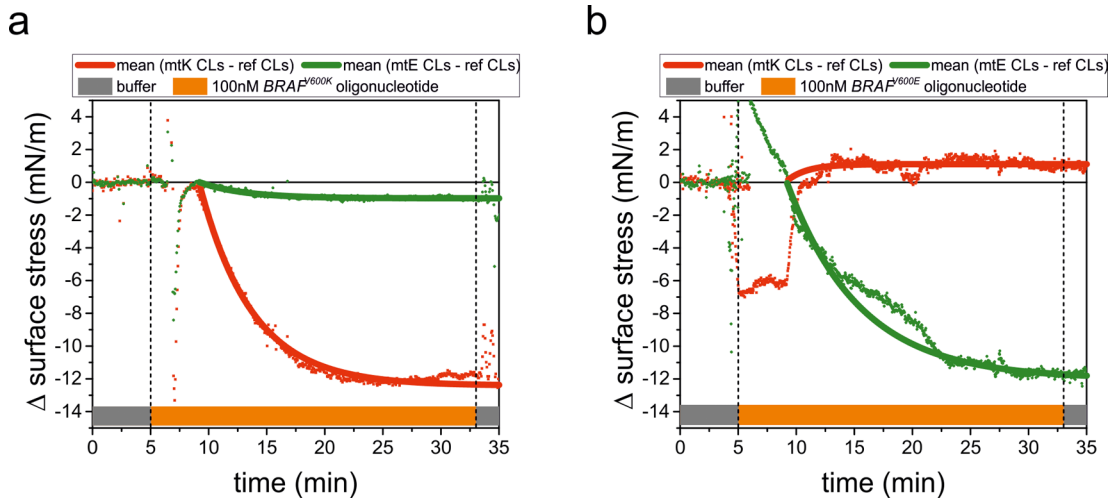

Figure 4. Analysis of $BRAF^{V600K}$ mutation using BRAFV600K and BRAFV600E complement oligonucleotides. Microcantilevers were functionalized with BRAFV600 K, BRAFV600E, and polyAC oligonucleotide. Shown in red: response difference between mutant BRAFV600 K and polyAC reference. Shown in green: response difference between mutant BRAFV600E and polyAC reference. Smooth lines represent Langmuir fits (R^2 > 0.95). (a) Injection of 100 nM BRAFV600 K complement and (b) 100 nM BRAFV600E complement.

containing the $BRAF^{V600E}$ mutation, and is comparable to the most sensitive sequencing methods currently in use.

Our method is capable of a more detailed mutation analysis. $BRAF^{V600K}$ is another less frequent mutation present in 10% of incidences. BRAFV600K oligonucleotide targets allow us to distinguish the $BRAF^{V600E}$ and $BRAF^{V600K}$ mutations. Exposing the corresponding cantilevers to BRAFV600K complements results in bending (Figure 4a), whereas the BRAFV600E cantilevers respond in the corresponding experiment with BRAFV600E complement (Figure 4b), emphasizing mutation discrimination. These experiments support the specificity of the assay and show the versatility of the cantilever array in investigating relevant multiple mutations simultaneously. The method does neither require PCR sample amplification nor labeling due to the fact that total RNA is used. Faster recognition of multiple mutations is achieved using parallel measurements owing to microcantilever arrays.

The proposed method has the following advantages: (1) Neither PCR sample amplification nor labeling is necessary due to the fact that total RNA is employed; (2) the technique avoids costly sample preparation steps; (3) the array format allows parallel simultaneous interrogation of multiple targetable mutations for an efficient analysis in one assay; (4) both fresh and routine paraffin embedded tissue (a single 20 μm thick slice) may be used; and (5) the high sensitivity is equivalent to the current sequencing technologies.

Here, the aim was to study BRAF mutations in melanoma. However, nanomechanical cantilevers may also be used for the detection of any point mutation, like BRCA1 and BRCA2 gene mutations in breast cancer. Another important breast cancer marker that is used to make treatment decisions is HER2. The HER2 gene is amplified which results in multiple copies of the gene as well as in increased expression of the HER2 protein. In a preliminary study, we already detected the amplified gene using specific oligonucleotide probes to demonstrate the versatility of our method. Moreover, protein overexpression is likely to be assessed using specific antibodies, reducing two different detection methods into one single microcantilever based assay. Gene mutation and protein expression analysis is also applicable to CRISPR/CAS9 gene editing, as insertions and deletions down to single point mutations can be easily verified, underlining the potential of the microcantilever technology.

■ ASSOCIATED CONTENT

Supporting Information

The Supporting Information is available free of charge on the ACS Publications website at DOI: 10.1021/acs.nanolett.6b01513.

Methods, table S1, and figures (Figures S1 and S2) (PDF)

■ AUTHOR INFORMATION

Corresponding Authors

*E-mail: francois.huber@unibas.ch.
*E-mail: christoph.gerber@unibas.ch.

Author Contributions

The study was conceived by F.H., H.P.L., K.G., and C.G. The experiments were designed and interpreted by F.H. and K.G. The experiments were performed and analyzed by F.H. DNA/RNA samples were prepared by K.G. and D.R. Cantilever arrays were prepared by H.P.L. and F.H. The manuscript was written by F.H., K.G., H.P.L., C.G., and E.M. All authors participated in the discussion of results and contributed valuable comments.

Funding

This work was funded by Swiss National Science Foundation, NanoTera Program (No. 20NA21_150957).

Notes

The authors declare no competing financial interest.

■ ACKNOWLEDGMENTS

We acknowledge valuable support from Michel Despont (formerly at IBM Research GmbH, Rüschlikon, now at CSEM SA, Neuchâtel, Switzerland) and Ute Drechsler (IBM Research GmbH, Rüschlikon, Switzerland) contributing cantilever arrays. The SNSF (Swiss National Science Foundation) scientifically evaluated the work financed by the Swiss Confederation and funded by Nano-Tera.ch. We thank the Swiss Nanoscience Institute (SNI) and the Cleven Foundation.

DOI: 10.1021/acs.nanolett.6b01513
Nano Lett. 2016, 16, 5373−5377

We further are grateful to Valeria Perrina (Institute of Pathology, University Hospital of Basel, Switzerland), the Zumbühl group, and the electronic and mechanical workshops (Department of Physics, University of Basel, Switzerland) for excellent technical assistance.

■ ABBREVIATIONS

BRAF Rapid Acceleration of Fibrosarcoma gene B

■ REFERENCES

(1) Ferlay, J.; Soerjomataram, I.; Dikshit, R.; Eser, S.; Mathers, C.; Rebelo, M.; Parkin, D. M.; Forman, D.; Bray, F. *Int. J. Cancer* **2015**, *136*, E359−E386.
(2) Simões, M. C. F.; Sousa, J. J. S.; Pais, A. A. C. C. *Cancer Lett.* **2015**, *357*, 8−42.
(3) Ravnan, M. C.; Matalka, M. S. *Clin. Ther.* **2012**, *34*, 1474−1486.
(4) Akbani, R.; Akdemir, K. C.; Aksoy, B. A.; Albert, M.; Ally, A.; Amin, S. B.; Arachchi, H.; Arora, A.; Auman, J. T.; Ayala, B.; et al. *Cell* **2015**, *161*, 1681−1696.
(5) Hatzivassiliou, G.; Haling, J. R.; Chen, H.; Song, K.; Price, S.; Heald, R.; Hewitt, J. F. M.; Zak, M.; Peck, A.; Orr, C.; et al. *Nature* **2013**, *501*, 232−236.
(6) Larkin, J. M. G.; Yan, Y. B.; McArthur, G. A.; Ascierto, P. A.; Liszkay, G.; Maio, M.; Mandala, M.; Demidov, L. V.; Stroyakovskiy, D.; Thomas, L.; et al. *J. Clin. Oncol.* **2015**, *33* (suppl. S), 9006.
(7) Lenz, T. L.; Becker, S. *Gene* **2008**, *427*, 117−123.
(8) Binnig, G.; Quate, C. F.; Gerber, C. *Phys. Rev. Lett.* **1986**, *56*, 930−933.
(9) Fritz, J.; Baller, M. K.; Lang, H. P.; Rothuizen, H.; Vettiger, P.; Meyer, E.; Güntherodt, H.-J.; Gerber, C.; Gimzewski, J. K. *Science* **2000**, *288*, 316−318.
(10) Hansen, K. M.; Ji, H.-F.; Wu, G.; Datar, R.; Cote, R.; Majumdar, A.; Thundat, T. *Anal. Chem.* **2001**, *73*, 1567−1571.
(11) McKendry, R.; Zhang, J.; Arntz, Y.; Strunz, T.; Hegner, M.; Lang, H. P.; Baller, M. K.; Certa, U.; Meyer, E.; Güntherodt, H.-J.; Gerber, C. *Proc. Natl. Acad. Sci. U. S. A.* **2002**, *99*, 9783−9788.
(12) Alvarez, M.; Carrascosa, L. G.; Moreno, M.; Calle, A.; Zaballos, Á.; Lechuga, L. M.; Martínez-A, C.; Tamayo, J. *Langmuir* **2004**, *20*, 9663−9668.
(13) Arntz, Y.; Seelig, J. D.; Lang, H. P.; Zhang, J.; Hunziker, P.; Ramseyer, J. P.; Meyer, E.; Hegner, M.; Gerber, C. *Nanotechnology* **2003**, *14*, 86−90.
(14) Backmann, N.; Zahnd, C.; Huber, F.; Bietsch, A.; Plückthun, A.; Lang, H. P.; Güntherodt, H.-J.; Hegner, M.; Gerber, C. *Proc. Natl. Acad. Sci. U. S. A.* **2005**, *102*, 14587−14592.
(15) Huber, F.; Hegner, M.; Gerber, C.; Güntherodt, H.-J.; Lang, H. P. *Biosens. Bioelectron.* **2006**, *21*, 1599−1605.
(16) Longo, G.; Alonso-Sarduy, L.; Rio, L. M.; Bizzini, A.; Trampuz, A.; Notz, J.; Dietler, G.; Kasas, S. *Nat. Nanotechnol.* **2013**, *8*, 522−526.
(17) Zhang, J.; Lang, H. P.; Huber, F.; Bietsch, A.; Grange, W.; Certa, U.; McKendry, R.; Güntherodt, H.-J.; Hegner, M.; Gerber, C. *Nat. Nanotechnol.* **2006**, *1*, 214−220.
(18) Huber, F.; Lang, H. P.; Backmann, N.; Rimoldi, D.; Gerber, C. *Nat. Nanotechnol.* **2013**, *8*, 125−129.
(19) Braun, T.; Backmann, N.; Vögtli, M.; Bietsch, A.; Engel, A.; Lang, H. P.; Gerber, C.; Hegner, M. *Biophys. J.* **2006**, *90*, 2970−2977.
(20) Barone, F.; Cellai, L.; Matzeu, M.; Mazzei, F.; Pedone, F. *Biophys. Chem.* **2000**, *86*, 37−47.
(21) Benson, D. A.; Karsch-Mizrachi, I.; Lipman, D. J.; Ostell, J.; Sayers, E. W. *Nucleic Acids Res.* **2011**, *39*, D32−D37.
(22) Halait, H.; DeMartin, K.; Shah, S.; Soviero, S.; Langland, R.; Cheng, S.; Hillman, G.; Wu, L.; Lawrence, H. J. *Diagn. Mol. Pathol.* **2012**, *21*, 1−8.
(23) Quintana, E.; Shackleton, M.; Foster, H. R.; Fullen, D. R.; Sabel, M. S.; Johnson, T. M.; Morrison, S. J. *Cancer Cell* **2010**, *18*, 510−523.

DOI: 10.1021/acs.nanolett.6b01513
Nano Lett. 2016, 16, 5373−5377